

# Large Scale Fabrication of Periodical Bowl-like Micropatterns of Single Crystal ZnO

Ding Lan,<sup>†</sup> Yuren Wang,<sup>\*,†</sup> Xiaolong Du,<sup>\*,‡</sup> Zengxia Mei,<sup>‡</sup> Qikun Xue,<sup>‡</sup> Ke Wang,<sup>§</sup> Xiaodong Han,<sup>§,||</sup> and Ze Zhang<sup>§,||</sup>

National Microgravity Laboratory, Institute of Mechanics, Chinese Academy of Sciences, Beijing 100190, China, Beijing National Laboratory for Condensed Matter Physics, Institute of Physics, Chinese Academy of Sciences, Beijing 100190, China, Institute of Microstructure and Property of Advanced Materials, Beijing University of Technology, Beijing 100022, China, and National Center of Electron Microscope, Beijing, 100080, China

Received December 25, 2007; Revised Manuscript Received May 21, 2008

**ABSTRACT:** Nanostructured ZnO materials are of great significance for their potential applications in photoelectronic devices, light-emitting displays, catalysis and gas sensors. In this paper, we report a new method to produce large area periodical bowl-like micropatterns of single crystal ZnO through aqueous-phase epitaxial growth on a ZnO single crystal substrate. A self-assembled monolayer of polystyrene microspheres was used as a template to confine the epitaxial growth of single crystal ZnO from the substrate, while the growth morphology was well controlled by citrate anions. Moreover, it was found that the self-assembled monolayer of colloidal spheres plays an important role in reduction of the defect density in the epitaxial ZnO layer. Though the mechanism is still open for further investigation, the present result indicates a new route to suppress the dislocations in the fabrication of single crystal ZnO film. A predictable application of this new method is for the fabrication of two-dimensional photonic crystal structures on light emitting diode surfaces.

Nanostructured ZnO materials have been extensively studied due to their potential applications in photoelectronic devices, light-emitting displays, catalysis and gas sensors. Many kinds of ZnO nanostructures, such as nanoflowers,<sup>1</sup> nanorods<sup>2,3</sup> and nanotetrapods,<sup>4,5</sup> are reported in the literature. More complex nanostructured ZnO films were fabricated by utilizing a sequential nucleation and growth method.<sup>6</sup> A new trend is to integrate individual nanostructured ZnO blocks into a large highly ordered assembly which is crucial for achieving adequate device performance. Hsu et al.<sup>7</sup> reported the fabrication of hierarchical micropatterns by the selective growth of ZnO nanocrystals. By utilizing a self-assembled microsphere monolayer as a template, periodic ZnO nanorod arrays<sup>8</sup> were successfully obtained. Bowl-like microstructured ZnO and TiO<sub>2</sub> were also reported in the literature,<sup>9–11</sup> in which the methods of nanoparticles/colloidal spheres codeposition, electrochemical deposition and atomic layer deposition were used to construct the bowl-like porous skeletons. In order to get periodic structures, controlling nucleation sites and growth morphology are important. Several methods<sup>12–14</sup> have been put forward to produce large area ZnO nanorod arrays through fluid flow driven self-assembly or growth on patterned Si substrate. A few researchers<sup>15,16</sup> reported the synthesis of single-crystalline patterned ZnO structure through solution-based epitaxial growth. In this paper, we report a new method to produce large area periodical bowl-like micropatterns (PBLM) of single crystal ZnO through aqueous-phase epitaxial growth on a ZnO single crystal substrate. A self-assembled monolayer of polystyrene (PS) microspheres was used as a template to confine the epitaxial growth of single crystal ZnO from the substrate and form

PBLM. Citrate anions were employed to control the growth morphology which was proven to be crucial to obtain the presented micropattern. On the basis of the knowledge of the authors, this is the first time for a report on the synthesis of such a micropattern of single crystal ZnO.

It is well-known that the light-emitting efficiency of a light-emitting diode (LED) is greatly limited by the internal reflection of the emitting light at the solid/air interface. It has been demonstrated that constructing photonic crystal (PC) structures<sup>17–23</sup> on the LED surface is a promising way to solve the problem. The present study provided a simple route to construct two-dimensional PC structure on the surface of single crystal ZnO substrate. Moreover, our method is based on an aqueous-phase synthesis of nanostructured ZnO and a totally chemical procedure for the preparation of patterned substrate. It offers the potential for low-cost, industrial-scale manufacturing<sup>6</sup> of PC-assistant LED devices. In addition, it was surprisingly revealed that the PS monolayer, which was used as a template for subsequent epitaxial growth, can obviously reduce the defect density and obtain high-quality epitaxial film. Different from the extensively reported “window” effect and lateral epitaxial overgrowth (LEO) technique by which threading dislocations could be suppressed,<sup>15,16</sup> the confinement effect of adjacent PS spheres may provide a new mechanism for efficiently reducing defect density in the epitaxial ZnO thin film.

Figure 1 shows a schematic of our experimental procedure. The single crystalline ZnO(0001) films with Zn-polarity were grown on Si(111) wafers by molecular beam epitaxy (MBE)<sup>24</sup> and were used as seeds in the subsequent hydrothermal growth of micropatterned ZnO film. The thickness of the MBE-grown ZnO film was 900 nm. PSs (10% in water) with a diameter of 1  $\mu\text{m}$  and 583 nm were self-assembled to make a monolayer mask<sup>25</sup> on the MBE-grown ZnO(0001)/Si(111) template. Then the substrate was heated at 90  $^{\circ}\text{C}$  for 15 min to sinter the colloidal spheres before the hydrothermal growth. The prepared monolayers of PSs were used as template film, which is shown in Figure 1I. The specimen was mounted upside-down in a

\* Correspondence should be addressed to (Y.W.) E-mail: wangyr@imech.ac.cn. Phone: +086-010-82544091. Fax: +086-010-82544096. (X.D.) E-mail: xlidu@aphy.iphy.ac.cn. Phone: +086-010-82649035. Fax: +086-010-82649228.

<sup>†</sup> Institute of Mechanics, Chinese Academy of Sciences.

<sup>‡</sup> Beijing National Laboratory for Condensed Matter Physics, Institute of Physics, Chinese Academy of Sciences.

<sup>§</sup> Beijing University of Technology.

<sup>||</sup> National Center of Electron Microscope.

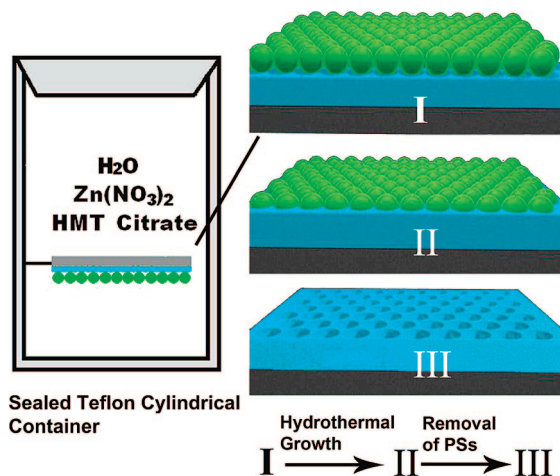


**Figure 1.** A schematic of the experimental procedure. The left panel shows the reaction container, the components of the precursor, and the status of the substrate; the brief fabrication procedure of ordered porous single crystal ZnO is shown in the right panel.

sealed Teflon cylindrical container, containing a 30-mL solution of 0.3 M methenamine ( $\text{C}_6\text{H}_{12}\text{N}_4$ , HMT), 0.03 M zinc nitrate hexahydrate ( $\text{Zn}(\text{NO}_3)_2 \cdot 6\text{H}_2\text{O}$ ) and 1.5 mg of sodium citrate. The reaction temperature and time are 60 °C and 36 h, respectively. The chemical reaction procedure was described in the literature.<sup>26</sup> The growth thickness can be controlled by the hydrothermal growth time. ZnO growth in the hydrothermal crucible was carefully controlled so as to enhance permeation of precursor solution and nucleation of ZnO in the interstitial space among the PSs of template film. Therefore, the PSs were buried in the as-grown single-crystal ZnO, which is shown schematically in Figure III. After removal of the PSs (burnt off at 450 ° or dissolved in toluene), the periodical bowl-like single-crystal ZnO film could be obtained, which is shown schematically in Figure III.

Figure 2a–c shows the SEM images of the synthesized ZnO film of PBLM. The hydrothermal growth was carried out for 36 h at the growth temperature of 60 °C. When the growth process was finished, the PSs were burnt off and left bowl-like air pores in the grown film. Figure 2a clearly shows that the air pores are arranged in a close-packed hexagonal-pattern, while the surface of the PBLM film was kept flat and smooth. To reveal the fine structure of PBLM film, the magnification SEM image is shown in Figure 2b. Due to the close-packing of the PSs, the air pores are tightly connected to each other through the small tunnels between two adjacent air pores. The cross-sectional SEM image of the sample is shown in Figure 2c. The image shows that the top porous layer integrated into the seed substrate very well. Almost no interface between the porous layer and the seed substrate could be distinguished on the image. It indicated that the epitaxial growth of single crystal ZnO was achieved. The diameter of the air pores is 1030 nm, which is consistent with the size of the PSs. This implies that no obvious shrinkage occurred in the synthesis of the porous film.

In the above procedure, a key issue is how to keep growth of ZnO homogeneous and smooth in the interstitial space among PSs during the growing process. It is well-known that ZnO grows rapidly in the [0001] direction. The growth rate of ZnO crystal should be well controlled in the experiment. The interstitial space among PSs can be divided into two parts, as shown in Figure 3a. It should be noted that the interstitial space is only several nanometers. Part I region is exposed to the solution directly.  $\text{Zn}^{2+}$  and HMT in the solution can readily

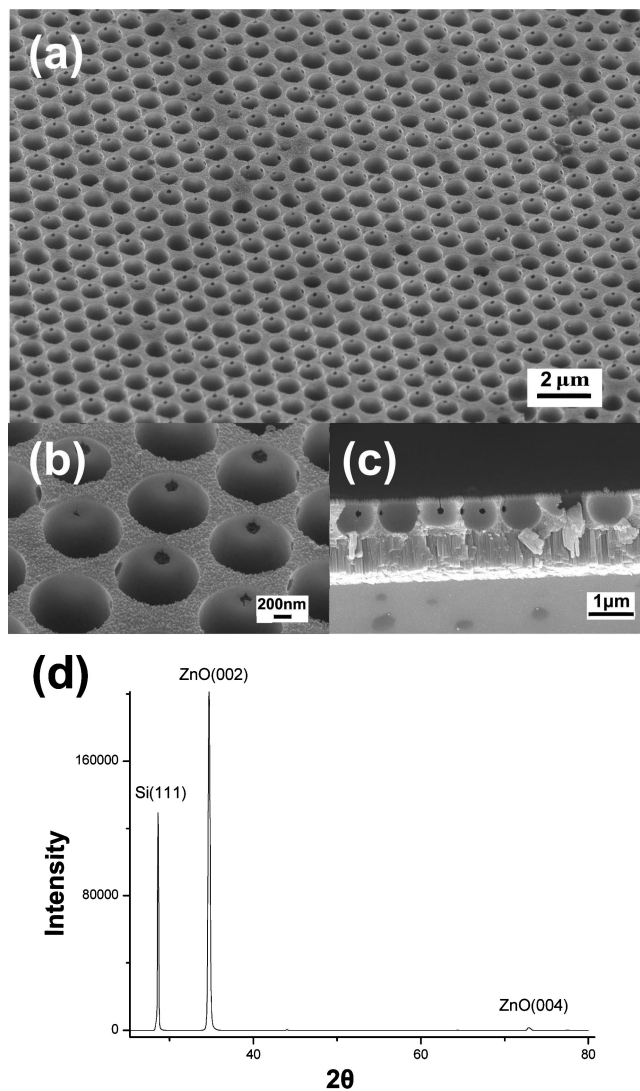


**Figure 2.** SEM images of a periodical bowl-like micropattern on single crystal ZnO substrate with PSs of 1 μm as the template. (a) The surface morphology with the citrate as the growth rate buffer agent. The hydrothermal growth time and the temperature are 36 h and 60 °C, respectively. (b) Magnification SEM image of (a), (c) cross-sectional SEM image of (a), (d) X-ray diffraction spectrum of (a).

diffuse to this region. On the contrary, part II region is shadowed by the PSs. Therefore, it is difficult for the solute to enter this region. Figure 3b shows the projection areas of part I and part II on the seed substrate. It is easy to understand that the easy diffusion of solute into region I induced the leading growth on the part I' region of the substrate prior to the part II' region. Figure 3c,d shows the SEM images of the sample growing in the precursor solution without adding sodium citrate. The surface morphology of the sample is ragged. This implied that the growth rate in region I' is much faster than that in region II'. Once the crystal growth in region I' approaches the pore throat, it will further hinder the solute diffusion into the niche surrounded by three close-packed PS spheres. The crystal growth in region II' was seriously suppressed. In order to solve the problem, it is necessary to suppress the growth in the ZnO [0001] direction so that the precursor solution can diffuse into the part II region. It has been demonstrated that citrate anions can control the crystal morphologies by adsorbing strongly on mineral surfaces<sup>27</sup> and altering the mineral growth behavior.<sup>28</sup> The citrate ions are absorbed preferentially on the (0001) surface

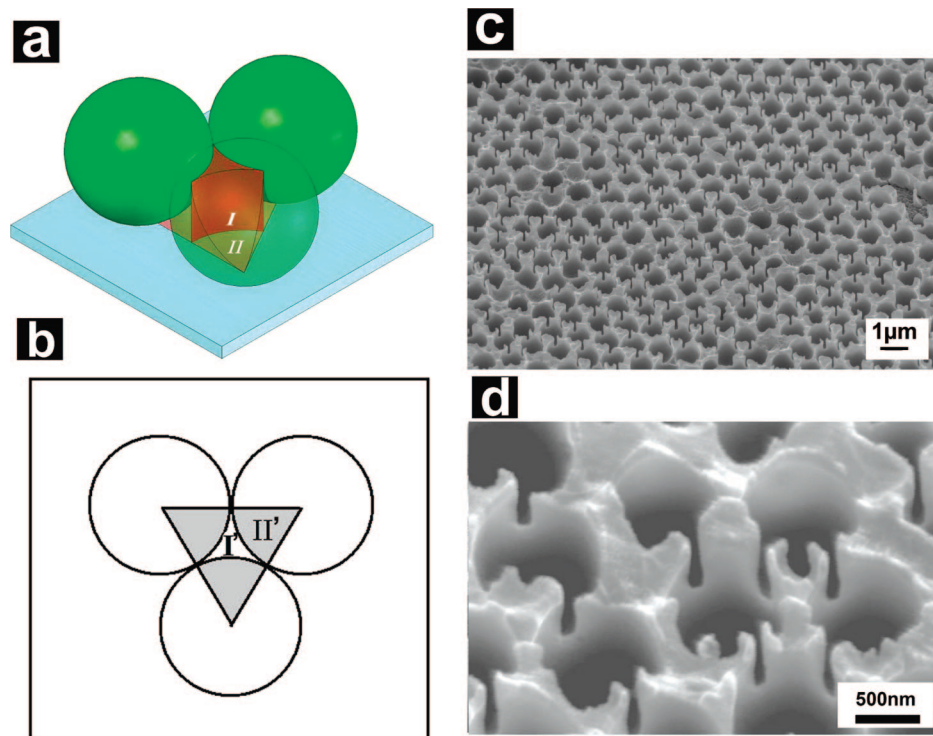


**Figure 3.** The nanospace and its effect on the epitaxial growth of ZnO. (a) The nanospace confined by substrate and PSs. (b) Two regions of the seed substrate for ZnO growth, (c) the sample that grew hydrothermally in the precursor solution without sodium citrate, (d) magnification of (c).

of ZnO and thus inhibit the crystal growth along the [0001] orientations.<sup>29</sup> In the experiment, we added a suitable amount of citrate in the solution to slow down the crystal growth along the [0001] orientation. The quality of the single-crystal porous ZnO film is improved remarkably (as shown in Figure 2a). Adding citrate ions into the precursor solution made the crystal growth in the pore niche more homogeneous.

We studied the crystal structure of the synthesized porous ZnO film by X-ray diffraction spectra (XRD), which is shown in Figure 2d. It can be seen that only diffraction peaks belonging to ZnO [001] reflections appeared on the XRD spectra, which is very consistent with the normal XRD spectra from single crystal ZnO film. It demonstrated that the porous ZnO film preserved the single crystal structure of the seed substrate and strongly orientated in the [0001] direction, even if the PS template was used in the hydrothermal growth.

TEM and high-resolution electron microscopy (HREM) experiments were used to characterize the microstructural features of the two epitaxial ZnO layers, parent epitaxial layer (P) and the daughter epitaxial layer (D), at the atomic scale. Figure 4a is a low magnification image of the ZnO thin film covered with a monolayer of PSs. The parent ZnO layer is indicated by 1 and the daughter epitaxial ZnO thin film is indicated by 2. An obvious interface between zone 1 and zone 2 was observed as indicated by the white dash line in Figure 4a. The selected area diffraction patterns taken from areas B, C and D are shown as b, c and d, respectively. It reveals that the parent epitaxial layer is single crystalline ZnO on Si substrate. The epitaxial growth is with an orientation relationship of  $(0001)_{\text{ZnO}} \parallel (\bar{1}\bar{1}\bar{1})_{\text{Si}}$  and  $[2\bar{1}\bar{1}0]_{\text{ZnO}} \parallel [011]_{\text{Si}}$ . The HREM image shown in Figure 4e (taken from the framed region E of Figure 4a) reveals that the features of parent epitaxial layer is high quality single crystalline ZnO film. The parent ZnO film shows excellent epitaxial characters at the atomic scale. The white dots can be regarded as atomic

chain projects according to the electron diffraction theory<sup>30</sup> with a first-order approximation. The simulated HREM image and the corresponding experimentally recorded HREM image are shown as insets in Figure 4e and they agree with each other very well. The parent epitaxial layer was through two transition layers as indicated as SiO<sub>x</sub> which is typical in conventional MBE growth of oxides on Si substrate.<sup>31</sup> It is noteworthy to pay attention to the “column-like” contrast in the parent epitaxial ZnO thin film layer. This column-like contrast terminates at the interface with the daughter ZnO epitaxial layer. The column-like contrast is suggested to derive from elastic field strains. No high or low angle grain boundaries were revealed in these column-like ZnO thin films. Figure 4f–h shows the HREM images of the 2D macroporous daughter epitaxial ZnO thin film which were hydrothermally grown on the MBE-grown parent ZnO template. The fast Fourier transformation (FFT) diffraction patterns are shown in the corresponding figures. The enlarged HREM images (Figure 4f–h) show the structural details of the framed areas F, G, H respectively in Figure 4a at the atomic level. Area H in Figure 4a contains the parent–daughter ZnO interface zone and shows the nucleation and transition characters of the daughter ZnO thin film on the parent. Figure 4h shows the microstructural characters of the transition zone which indicates heavy lattice distortions. The interface transition zone is about 50–100 nm thick. Through this interface transition zone, the strain was released quickly and the up-grown ZnO thin films show high quality single crystalline features. Across the parent–daughter interface, the column-like contrast in the parent zone disappeared sharply. As revealed in Figure 4f (the side of the PS) and Figure 4g (the bottom of the PS), both PS/ZnO interface regions (bottom and side) show very high quality single crystalline ZnO characters. The above results suggest that the PS monolayer suppressed the formation of threading defects or released the

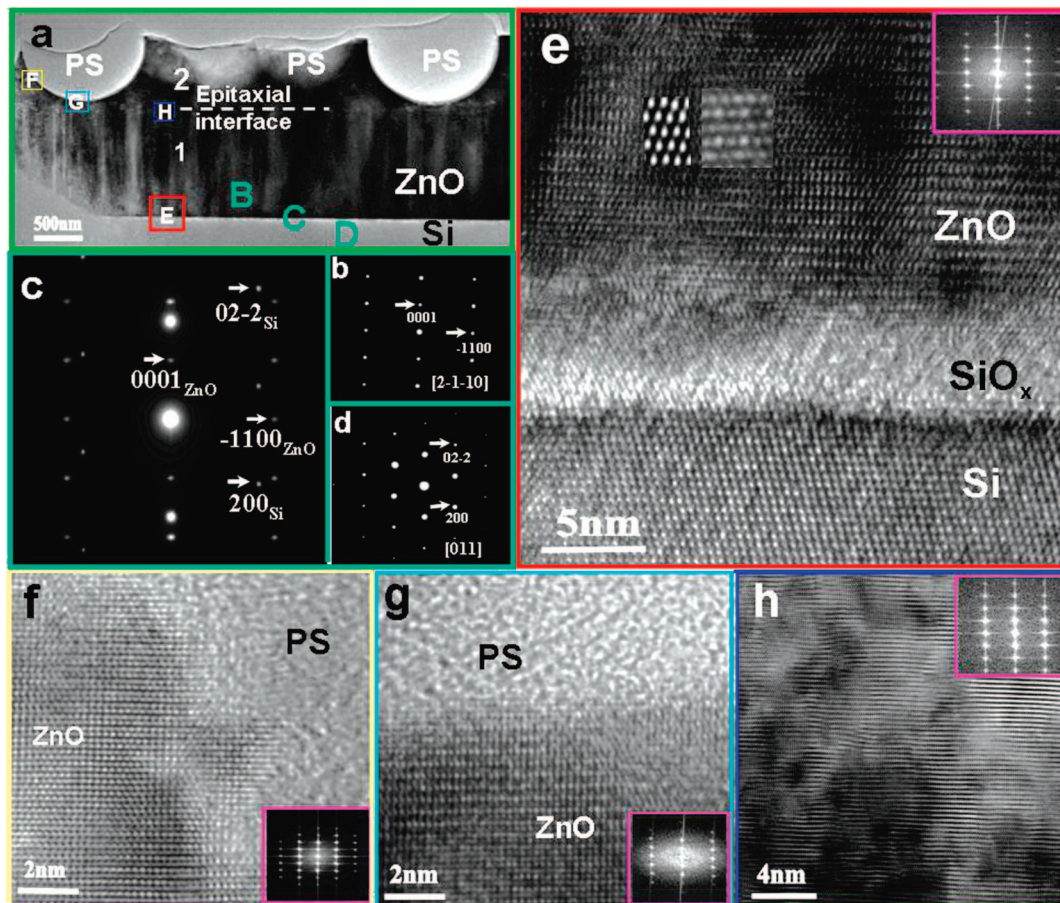


**Figure 4.** (a) TEM image shows the interface region between the epitaxial ZnO layer of the bowl-like micropattern and the seed single crystal ZnO film grown on a silicon (111) substrate. The selected area diffraction patterns corresponding to B, C, and D marked regions in image (a) were shown in panels (b), (c) and (d), separately. High-resolution electron microscopy (HREM) images corresponding to E, F, G and H marked regions in image (a) were shown in panels (e), (f), (g) and (h), respectively.

threading defects along the PS interface in the hydrothermally grown ZnO film. Interestingly, almost perfect ZnO/PS interface without any detectable line defects at the atomic scale indicates the extreme benign interface structure of the PS for ZnO ordering growth. These results suggested the threading dislocations in LEO mode are bent to and/or confined in the masked region due to the change of growth direction from vertical to lateral.<sup>32</sup> Therefore, window region itself in the LEO mode just provided a passage for the subsequent epitaxial growth and has no effect on the defect reduction. In fact, defects directly go through the window region and extend to the up-grown epitaxial region in ZnO LEO,<sup>15</sup> while much less threading defects were observed in the overgrown wing area. For this reason, the second growth and interlaced windows were used in ZnO LEO to guarantee a homogeneous low-defect growth. It seems that the colloidal sphere monolayer used in our experiment can be regarded as periodical mask in LEO. However, it is noteworthy that the high quality single crystal porous film was grown in the interstitial sites among the close packed colloidal spheres, other than overgrowth from the colloidal sphere monolayer. Therefore, the lateral growth mechanism cannot be used to explain the defect reduction observed in our experiment. The interstitial site surrounded by three close packed colloidal spheres has a complicated geometrical shape, as shown schematically in Figure 3a. It has nanometer-sized dimension which strongly limited solvent diffusion and selective nucleation in the epitaxial growth. It is suggested that the

defect reduction mechanism has a strong relationship to the nanospace-confined diffusion process and the selective nucleation procedure.

In summary, we developed a new method to produce the large area periodical bowl-like micropattern (PBLM) of single crystal ZnO through an aqueous-phase epitaxial growth on a ZnO single crystal substrate. Self-assembled monolayer of polystyrene microspheres was used as a template to confine the epitaxial growth of single crystal ZnO from the substrate, while the growth morphology was well controlled by citrate anions. Moreover, the self-assembled monolayer of colloidal spheres plays an important role in reduction of the defect density in the epitaxial ZnO layer. Though the mechanism is still open for further investigation, the present result indicates a new route to suppress the dislocations in the fabrication of single crystal ZnO film. A predicable application of this new method is the fabrication of 2D photonic crystal structures on LED surfaces.

**Acknowledgment.** This project is supported by the Knowledge Innovation Program of the Chinese Academy of Sciences (Grant No KJCX2-SW-L05) and The National Science Foundation of China (Grant No 50532090).

**Supporting Information Available:** Fabrication of single crystal ZnO substrate, overgrowth of the periodical bowl-like single-crystal ZnO, the periodical bowl-like single-crystal ZnO of 583 nm and characterization of the experiments. This material is available free of charge via the Internet at <http://pubs.acs.org>.

## References

- (1) Wang, Z.; Qian, X. F.; Yin, J.; Zhu, Z. K. Large-scale fabrication of tower-like, flower-like, and tube-like ZnO arrays by a simple chemical solution route. *Langmuir* **2004**, *20* (8), 3441–3448.
- (2) Choy, J. H.; Jang, E. S.; Won, J. H.; Chung, J. H.; Jang, D. J.; Kim, Y. W. Soft solution route to directionally grown ZnO nanorod arrays on Si wafer; room-temperature ultraviolet laser. *Adv. Mater.* **2003**, *15* (22), 1911–1914.
- (3) Park, W. I.; Yi, G. C.; Kim, J. W.; Park, S. M. Schottky nanocontacts on ZnO nanorod arrays. *Appl. Phys. Lett.* **2003**, *82* (24), 4358–4360.
- (4) Newton, M. C.; Warburton, P. A. ZnO tetrapod nanocrystals. *Mater. Today* **2007**, *10* (5), 50–54.
- (5) Chen, Z.; Shan, Z. W.; Cao, M. S.; Lu, L.; Mao, S. X. Zinc oxide nanotetrapods. *Nanotechnology* **2004**, *15* (3), 365–369.
- (6) Sounart, T. L.; Liu, J.; Voigt, J. A.; Hsu, J. W.; Spoerke, E. D.; Tian, Z.; Jiang, Y. B. Sequential nucleation and growth of complex nanostructured films. *Adv. Funct. Mater.* **2006**, *16* (3), 335–344.
- (7) Hsu, J. W.; Tian, Z. R.; Simmons, N. C.; Matzke, C. M.; Voigt, J. A.; Liu, J. Directed spatial organization of zinc oxide nanorods. *Nano Lett.* **2005**, *5* (1), 83–86.
- (8) Liu, D. F.; Xiang, Y. J.; Wu, X. C.; Zhang, Z. X.; Liu, L. F.; Song, L.; Zhao, X. W.; Luo, S. D.; Ma, W. J.; Shen, J.; Zhou, W. Y.; Wang, G.; Wang, C. Y.; Xie, S. S. Periodic ZnO nanorod arrays defined by polystyrene microsphere self-assembled monolayers. *Nano Lett.* **2006**, *6* (10), 2375–2378.
- (9) Cao, B. Q.; Cai, W. P.; Sun, F. Q.; Li, Y.; Lei, Y.; Zhang, L. D. Fabrication of large-scale zinc oxide ordered pore arrays with controllable morphology. *Chem. Commun.* **2004**, *14*, 1604–1605.
- (10) Liu, Z. F.; Jin, Z. G.; Li, W.; Qiu, H. J. Assembly of ordered ZnO porous thin films by cooperative assembly method using polystyrene spheres and Ultrafine ZnO particles. *Mater. Res. Bull.* **2006**, *41* (1), 119–127.
- (11) Xu, D. W.; Graugnard, E.; King, J. S.; Zhong, L. W.; Summers, C. J. Large-scale fabrication of ordered nanobowl arrays. *Nano Lett.* **2004**, *4* (11), 2223–2226.
- (12) Sun, B. Q.; Siringhaus, H. Surface tension and fluid flow driven self-assembly of ordered ZnO nanorod films for high-performance field effect transistors. *J. Am. Chem. Soc.* **2006**, *128* (50), 16231–16237.
- (13) Kim, Y. J.; Lee, C. H.; Hong, Y. J.; Yi, G. C.; Kim, S. S.; Cheong, H. Controlled selective growth of ZnO nanorod and microrod arrays on Si substrates by a wet chemical method. *Appl. Phys. Lett.* **2006**, *89*, (16312816)
- (14) Tak, Y.; Yong, K. J. Controlled growth of well-aligned ZnO nanorod array using a novel solution method. *J. Phys. Chem. B* **2005**, *109* (41), 19263–19269.
- (15) Andeen, D.; Kim, J. H.; Lange, F. F.; Goh, G. K. L.; Tripathy, S. Lateral epitaxial overgrowth of ZnO in water at 90 degrees C. *Adv. Funct. Mater.* **2006**, *16*, 799–804.
- (16) Kim, J. H.; Andeen, D.; Lange, F. F. Hydrothermal growth of periodic, single-crystal ZnO microrods and microtunnels. *Adv. Mater.* **2006**, *18*, 2453.
- (17) Byeon, K. J.; Hwang, S. Y.; Lee, H. Fabrication of two-dimensional photonic crystal patterns on GaN-based light-emitting diodes using thermally curable monomer-based nanoimprint lithography. *Appl. Phys. Lett.* **2007**, *91*, (0911069)
- (18) Kim, S. H.; Lee, K. D.; Kim, J. Y.; Kwon, M. K.; Park, S. J. Fabrication of photonic crystal structures on light emitting diodes by nanoimprint lithography. *Nanotechnology* **2007**, *18*, (0553065)
- (19) Cho, H. K.; Jang, J.; Choi, J. H.; Choi, J.; Kim, J.; Lee, J. S.; Lee, B.; Choe, Y. H.; Lee, K. D.; Kim, S. H.; Lee, K.; Kim, S. K.; Lee, Y. H. Light extraction enhancement from nano-imprinted photonic crystal GaN-based blue light-emitting diodes. *Opt. Express* **2006**, *14* (19), 8654–8660.
- (20) Lin, C. H.; Tsai, J. Y.; Kao, C. C.; Kuo, H. C.; Yu, C. C.; Lo, J. R.; Leung, K. M. Enhanced light output in InGaN-based light-emitting diodes with omnidirectional one-dimensional photonic crystals. *Jpn. J. Appl. Phys. Part 1* **2006**, *45* (3A), 1591–1593.
- (21) Kim, D. H.; Cho, C. O.; Roh, Y. G.; Jeon, H.; Park, Y. S.; Cho, J.; Im, J. S.; Sone, C.; Park, Y.; Choi, W. J.; Park, Q. H. Enhanced light extraction from GaN-based light-emitting diodes with holographically generated two-dimensional photonic crystal patterns. *Appl. Phys. Lett.* **2005**, *87*, (20350820)
- (22) Wierer, J. J.; Krames, M. R.; Epler, J. E.; Gardner, N. F.; Craford, M. G.; Wendt, J. R.; Simmons, J. A.; Sigalas, M. M. InGaN/GaN quantum-well heterostructure light-emitting diodes employing photonic crystal structures. *Appl. Phys. Lett.* **2004**, *84* (19), 3885–3887.
- (23) Oder, T. N.; Kim, K. H.; Lin, J. Y.; Jiang, H. X. III-nitride blue and ultraviolet photonic crystal light emitting diodes. *Appl. Phys. Lett.* **2004**, *84* (4), 466–468.
- (24) Wang, X. N.; Wang, Y.; Mei, Z. X.; Dong, J.; Zeng, Z. Q.; Yuan, H. T.; Zhang, T. C.; Du, X. L.; Jia, J. F.; Xue, Q. K.; Zhang, X. N.; Zhang, Z.; Li, Z. F.; Lu, W. Low-temperature engineering for high-quality epitaxy of ZnO film on Si(111) substrate. *Appl. Phys. Lett.* **2007**, *90*, 151912.
- (25) Wang, X. D.; Summers, C. J.; Wang, Z. L. Large-scale hexagonal-patterned growth of aligned ZnO nanorods for nano-optoelectronics and nanosensor arrays. *Nano Lett.* **2004**, *4*, 423–426.
- (26) Vayssieres, L. Growth of arrayed nanorods and nanowires of ZnO from aqueous solutions. *Adv. Mater.* **2003**, *15*, 464–466.
- (27) Lopez-Macipe, A.; Gomez-Morales, J.; Rodriguez-Clemente, R. The role of pH in the adsorption of citrate ions on hydroxyapatite. *J. Colloid Interface Sci.* **1998**, *200*, 114–120.
- (28) Liu, C.; Huang, P. M. Atomic force microscopy and surface characteristics of iron oxides formed in citrate solutions. *Soil Sci. Soc. Am. J.* **1999**, *63*, 65–72.
- (29) Tian, Z. R. R. Complex and oriented ZnO nanostructures. *Nat. Mater.* **2003**, *2*, 821–826.
- (30) Cowley J. M. *Diffraction Physics*; North-Holland Publishing Company: New York, 1975.
- (31) Hu, X. M.; Li, H.; Liang, Y.; Wei, Y.; Yu, Z.; Marshall, D.; Edwards, J.; Droopad, R.; Zhang, X.; Demkov, A. A.; Moore, K.; Kulik, J. The interface of epitaxial SrTiO<sub>3</sub> on silicon: in situ and ex situ studies. *Appl. Phys. Lett.* **2003**, *82*, 203–205.
- (32) Tanaka, S.; Honda, Y.; Sawaki, N.; Hibino, M. Structural characterization of GaN laterally overgrown on a (111) Si substrate. *Appl. Phys. Lett.* **2001**, *79*, 955–957.

CG7012683